

Compact generation of easy-to-access continuous-variable cluster states

Ioannes Rigas,^{1,2,*} Christian Gabriel,^{1,2,*} Stefan Berg-Johansen,^{1,2} Andrea Aiello,^{1,2}
Peter van Loock,^{1,2,3} Ulrik L. Andersen,^{1,2,4} Christoph Marquardt,^{1,2,†} and Gerd Leuchs^{1,2}

¹Max Planck Institute for the Science of Light, Guenther-Scharowsky-Str. 1/Bldg. 24, D-91058 Erlangen, Germany

²Institute of Optics, Information and Photonics, University Erlangen-Nuremberg, Staudtstr. 7/B2, D-91058 Erlangen, Germany

³Institute of Physics, University of Mainz, Staudingerweg 7, 55128 Mainz, Germany

⁴Department of Physics, Technical University of Denmark, 2800 Kongens Lyngby, Denmark

Cluster states are an essential component in one-way quantum computation protocols. We present novel schemes to generate addressable and scalable cluster states. Specifically, we exploit the entanglement contained in quadrature squeezed cylindrically polarized modes as the resource for our cluster state production. We carefully examine the properties of the obtained cluster states and quantify these. It is shown that these cluster states can be built through very compact designs. All modes are directly addressable, as needed for one-way quantum computation. Furthermore, we experimentally implement one of the proposed schemes and verify its feasibility by measuring the quantum correlations between the different nodes of the cluster state.

PACS numbers: 03.67.Lx, 42.50.Dv, 03.65.Ud, 03.67.Bg

The efficient processing of computational tasks is extremely desirable in today's fast evolving information society. Quantum computers have the potential to clearly outperform classical systems at certain computational operations [1]. The necessary technologies for such a quantum computing device are slowly evolving, however, further improvements of these are essential before one can build an operational quantum computer.

It has been shown that so-called cluster states represent a universal resource for measurement-based, one-way quantum computation, which can be performed with discrete-variable (DV) systems [2–6] as well as with continuous-variable (CV) quantum states [7–12]. In these schemes specially prepared entangled states, the cluster states, form the backbone of the protocol. The central idea behind cluster-state quantum computation is to enact quantum logic gates on parts of an initially prepared cluster state by teleporting them through the cluster. These gates are then implemented solely by means of local measurements, while additional Hadamard (DV) or Fourier (CV) gates are built-in along the teleportations to switch between different bases and obtain universality. The first measurement results determine which bases to choose for the remaining measurements and which Pauli (DV) or displacement (CV) corrections to apply. Thus, in this model, the complication of implementing deterministic quantum gates is transferred to the task of generating highly non-locally correlated cluster states, typically, either in a probabilistic (DV) or deterministic (CV) fashion.

While it is possible to deterministically generate CV cluster states using squeezed light and linear optics [13], there are still difficulties to overcome with regards to scaling up such states to sufficiently many, addressable modes. The experimental realization of large cluster states still remains a major challenge and a reduction of the complexity of the setup is highly desirable if one wants to implement these states in a quantum computing protocol. A key element in the optical cluster-state generation process, determining how compact the cluster state will become, is the nonclassical state of light that serves as the

physical resource for the cluster. There are various approaches to this, for example, the use of optical frequency combs to generate CV cluster states [10–12, 14]. Such cluster states can be created in a very compact way which makes them potentially scalable. However, in these schemes, the addressability of each node of the cluster, as needed for quantum computation, still imposes a challenge. The alternate, linear-optics method [13] to obtain CV cluster states has been demonstrated in [15]. In this case, the resources for cluster-state generation are squeezed Gaussian modes combined at a network of beam splitters. While, in principle, any cluster topology can be achieved this way [13] and the different spatial modes that form the cluster are also easily addressable, a compact design in this approach is difficult. Alternatively, one may encode the cluster states in a temporal fashion by repeatedly reusing the same optical hardware [16, 17]. However, this kind of approach has the complication of implementing sufficiently long delay loops.

In this Letter, we report on a new scheme to generate cluster states with the help of quadrature squeezed cylindrically polarized modes. The presented cluster states rely on the four orthogonal basis modes of the cylindrically polarized states which can be easily distinguished and addressed. Moreover, this approach to cluster generation is very compact, since non-classical multi-mode correlations are obtained for all involved cylindrically polarized modes in a single nonlinear process. This could be for example a photonic crystal fiber [18, 19] or an optical parametric oscillator [20, 21]. The schemes proposed here are designed in such a way that they offer, at the same time, a compact and robust cluster-state preparation as well as an easy and direct addressability of the nodes of the cluster. At the end of this paper, we report on an experimental demonstration of one of the proposed schemes, for which we measure the quantum correlations present among all the four nodes of the cluster state.

For continuous variables, in the limit of infinite squeezing,

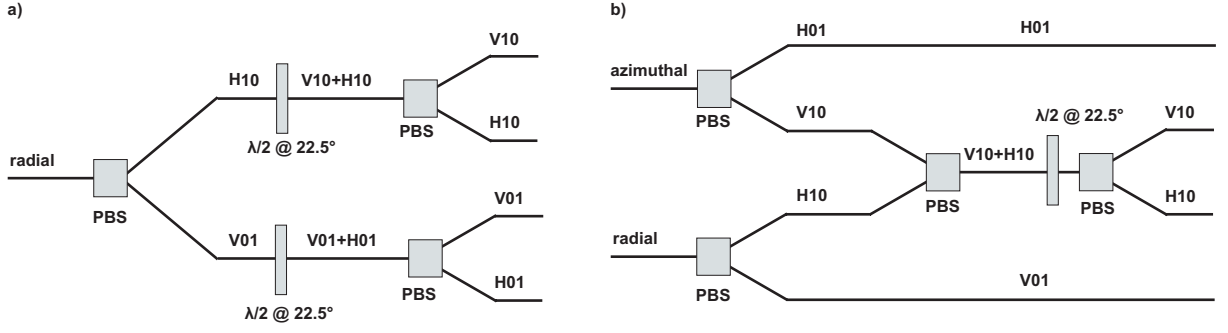


FIG. 1. In a) scheme 1 for cluster-state generation is presented. A radially polarized mode enters a linear-optics network with the four output modes then forming a cluster state. The radially polarized mode could also be substituted by an azimuthally polarized one to generate a similar cluster state. In b) scheme 2 is shown. One radially and one azimuthally polarized mode form the input state. The four output modes again constitute a cluster state. [polarizing beam splitter (PBS), half-wave plate ($\lambda/2$)].

cluster states fulfill the eigenequation [13]

$$\left(\hat{p}_j - \sum_{k \in N_j} A_{jk} \hat{q}_k\right) |\psi\rangle \rightarrow 0 \quad \forall j. \quad (1)$$

This is in analogy to the discrete case, where cluster states are eigenstates of the Pauli stabilizers $\hat{\sigma}_x^{(j)} \prod_{k \in N_j} \hat{\sigma}_z^{(k)}$ [22]. In the CV case, \hat{p}_j and \hat{q}_j correspond to the “position” and “momentum” operators of the optical mode j . N_j are the adjacent modes of the mode j . The real matrix \mathbf{A} contains the full information about the cluster or, equivalently, its graph. It therefore determines what the displacement corrections after measuring some of the modes must be in order to achieve, in principle, unit-fidelity teleportation. This is reflected by the fact that the covariances of the operators $(\hat{p}_j - \sum_k A_{jk} \hat{q}_k)$, which correspond to the excess noises acquired during the individual teleportation steps, all vanish. Note that in a two-mode scenario, the state that satisfies Eq. (1) is the famous EPR state up to a local Fourier rotation.

In any realistic scenario, however, one is limited to finitely squeezed input states. Thus, quantum teleportation using realistic cluster states always has non-unit fidelities, so that these physical clusters are non-ideal states for universal quantum computation. Nevertheless, one can define *approximate* cluster states or *Gaussian graph states* [23] which clearly specify the correlations between the individual modes in a cluster, as well as the infidelities of the quantum operations that have to be accepted for a finite degree of squeezing. The full information on any (zero-mean) Gaussian state is contained in its covariance matrix. CV cluster states can then be completely described by the adjacency matrices of their graphs [23], defined as,

$$\mathbf{Z} = i\mathbf{U} + \mathbf{V}. \quad (2)$$

Here, \mathbf{U} and \mathbf{V} are given by

$$\mathbf{U} = \frac{1}{2} \langle \hat{\mathbf{q}} \hat{\mathbf{q}}^T \rangle^{-1}, \quad \mathbf{V} = \langle \hat{\mathbf{q}} \hat{\mathbf{q}}^T \rangle^{-1} \times \langle \{\hat{\mathbf{q}}, \hat{\mathbf{p}}^T\} \rangle, \quad (3)$$

where $\langle \hat{\mathbf{q}} \hat{\mathbf{q}}^T \rangle$ denotes the position covariance matrix and $\langle \{\hat{\mathbf{q}}, \hat{\mathbf{p}}^T\} \rangle$ the matrix describing the cross-correlations between position and momentum, defined as $\langle \{\hat{\mathbf{q}}, \hat{\mathbf{p}}^T\} \rangle_{jk} = \frac{1}{2} \langle (\hat{q}_j \hat{p}_k + \hat{p}_k \hat{q}_j) \rangle$. The role of \mathbf{U} is to incorporate the finite squeezing of each mode, while \mathbf{V} represents the coupling between the modes. For the complex adjacency matrix \mathbf{Z} , replacing the real matrix \mathbf{A} , Eq. (1) becomes an exact zero-eigenequation even for finite squeezing [23]. It is therefore a convenient tool to quantify and describe finitely squeezed cluster states.

For a realistic cluster with finite squeezing, the complex adjacency matrix now determines both the necessary displacements during teleportation and the excess noise that inevitably will be added to the state after teleportation: the covariances of the operators $(\hat{p}_j - \sum_k V_{jk} \hat{q}_k)$ are given by the matrix elements $U_{nm}/2$, so that the total matrix \mathbf{Z} contains the full information on the intermode correlations of a cluster state.

Our cluster-state generation schemes are based on cylindrically polarized beams. These can be described by a superposition of two out of four distinct modes. If one chooses, for example, the Hermite-Gaussian basis to define cylindrically polarized modes, this would be the two first-order Hermite Gaussian TEM_{10} (10) and TEM_{01} (01) with horizontal (H) and vertical (V) polarization, namely $H10$, $V10$, $H01$ and $V01$ [24]. In [19] we have shown that by quadrature squeezing a cylindrically polarized beam, one generates squeezing in entanglement between the basis modes. Our cluster states rely precisely on these properties. The two most common cylindrically polarized modes are the radially and azimuthally polarized modes, described by the annihilation operators \hat{a}_R and \hat{a}_A , respectively. Their annihilation operators are defined as follows,

$$\hat{a}_R = \frac{1}{\sqrt{2}}(\hat{a}_{H10} + \hat{a}_{V01}), \quad \hat{a}_A = \frac{1}{\sqrt{2}}(\hat{a}_{V10} - \hat{a}_{H01}). \quad (4)$$

The entanglement-generating operation is modeled by the squeezing operator

$$\hat{S}(r, \theta) = \exp[r(e^{-i\theta} \hat{a}^2 - e^{i\theta} \hat{a}^{\dagger 2})/2], \quad (5)$$

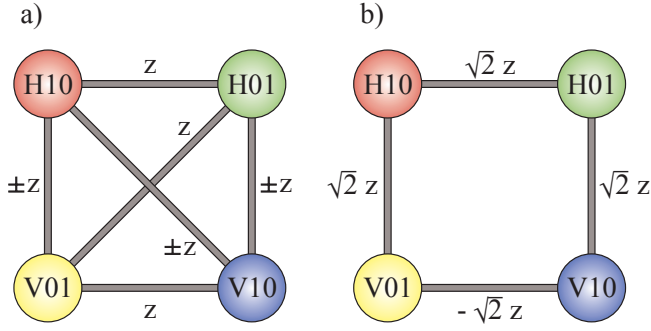


FIG. 2. The cluster states generated from scheme 1, displayed in a), and scheme 2, displayed in b). In scheme 1, a quadrature squeezed radially polarized mode is assumed as the input mode. The parameter z is related to the squeezing of the cylindrically polarized mode at the input and, in these plots, quantifies the strength of the entanglement between the different, individually addressable modes.

applied before the beam enters the passive circuit which generates the final cluster state.

In the present work, we propose two schemes to generate two different types of cluster states. A key element in both schemes are, on the one hand, polarizing beam splitters (PBSs), which act as mode separators and combiners and, on the other hand, half-wave plates orientated at 22.5° . These rotate the input state by $\hat{a}_{H/V} \mapsto (\hat{a}_H \pm \hat{a}_V)/\sqrt{2}$, thus performing a mode mixing between the different input modes.

The first scheme is illustrated in Fig. 1a). A quadrature squeezed azimuthally (or radially) polarized mode is sent through an array of PBSs and half-wave plates. These are configured in such a way that one gains access to all four basis modes which are spatially separated at the output of the circuit. In Scheme 2, displayed in Fig. 1b), quadrature squeezed azimuthally and radially polarized modes are split into their basis modes. In the next step one pair of orthogonally polarized modes is combined on a PBS and then mixed with a half-wave plate orientated at 22.5° . After the half-wave plate, the modes are separated again at a PBS, therefore allowing one to access all four basis modes in spatially separated arms.

In order to characterize the output states of the proposed schemes, we calculate their adjacency matrices, giving us the full information about any quantum correlations contained in these states. To do so, we make use of the fact that any unitary operation \hat{U} corresponding to a symplectic transformation $\hat{U}^\dagger \hat{\mathbf{x}} \hat{U} = \mathbf{S} \hat{\mathbf{x}}$ changes the covariance matrix \mathbf{C} of a Gaussian state according to

$$\hat{\rho} \mapsto \hat{U} \hat{\rho} \hat{U}^\dagger : \quad \mathbf{C}^\rho \mapsto \mathbf{S} \mathbf{C}^\rho \mathbf{S}^T. \quad (6)$$

For a complete theoretical description of the state, however, we do not only have to consider the co-rotating radially and azimuthally polarized modes, $\hat{a}_{R+} = \hat{a}_R$, $\hat{a}_{A+} = \hat{a}_A$, but also their counter-rotating complements, $\hat{a}_{A-} = (\hat{a}_{V10} + \hat{a}_{H01})/\sqrt{2}$, $\hat{a}_{R-} = (-\hat{a}_{H10} + \hat{a}_{V01})/\sqrt{2}$ [24].

The symplectic matrix for each cluster generation scheme is composed of the matrices of the individual squeezing and

passive elements. From the covariance matrix $\mathbf{C}^{\text{out}} = \frac{1}{2} \mathbf{S} \mathbf{S}^T$, one can then extract the adjacency matrix of each scheme according to (3). As a final result for the adjacency matrices describing the cluster graphs for schemes 1 and 2, we obtain

$$\begin{aligned} \mathbf{Z}_1^{A/R} &= i \mathbb{1}_4 + z \tilde{\mathbf{V}}_1^{A/R}, \\ \mathbf{Z}_2 &= 2(z + i) \mathbb{1}_4 + \sqrt{2} z \tilde{\mathbf{V}}_2, \end{aligned} \quad (7)$$

with

$$\tilde{\mathbf{V}}_1^{A/R} = \begin{pmatrix} 1 & \pm 1 & 1 & \pm 1 \\ \pm 1 & 1 & \pm 1 & 1 \\ 1 & \pm 1 & 1 & \pm 1 \\ \pm 1 & 1 & \pm 1 & 1 \end{pmatrix}, \quad \tilde{\mathbf{V}}_2 = \begin{pmatrix} 0 & 0 & 1 & 1 \\ 0 & 0 & 1 & -1 \\ 1 & 1 & 0 & 0 \\ 1 & -1 & 0 & 0 \end{pmatrix}.$$

Here, the first (last) two columns denote the beams with a TEM_{10} (TEM_{01}) spatial profile, while the odd (even) number channels correspond to horizontal (vertical) polarization. The superscripts A and R represent the case for the radial or azimuthal input mode in scheme 1, respectively. The parameter z quantifies the amount of squeezing of the input modes. It is related to the input squeezing in Eq. (5) as $z = (\langle \hat{q} \hat{p}_{\text{in}} \rangle - i \langle \hat{q}_{\text{in}}^2 \rangle + \frac{i}{2}) / 4 \langle \hat{q}_{\text{in}}^2 \rangle$, with $\langle \hat{q}_{\text{in}}^2 \rangle$ and $\langle \hat{q} \hat{p}_{\text{in}} \rangle$ being the (co-)variances of the input mode. For a squeezed input state, these two quantities are given by

$$\begin{aligned} \langle \hat{q}_{\text{in}}^2 \rangle &= \frac{1}{2} [\cosh(2r) - \sinh(2r) \cos \theta], \\ \langle \hat{q} \hat{p}_{\text{in}} \rangle &= -\frac{1}{2} \sinh(2r) \sin \theta. \end{aligned} \quad (8)$$

Here r is the degree of squeezing and θ the squeezing angle. The adjacency matrices clearly show that quantum correlations between the different modes exist and that the output states form a cluster. Especially intriguing is the form of the cluster's graph, showing which modes are directly entangled to each other. The topological structure of these states are displayed in Fig. 2. The cluster state obtained from scheme 1 has the unique feature that all modes are directly linked to each other, corresponding to a so-called fully connected graph. In the case of an azimuthally polarized input beam, it is even *fully symmetric* under permutation of its output modes. To our knowledge, an experimental generation of a fully symmetric and connected, optical cluster state has not been achieved yet, and we will discuss below our proof-of-principle experiment for this. The cluster state from scheme 2 displays a box-like structure. Cluster states with this graph topology have already proven their importance for quantum teleportation protocols, both experimentally and theoretically [13, 15].

Our cluster-state generation schemes are distinct from other schemes through the simplicity of their implementation. The cylindrically polarized modes, which form the backbone of the setups, can be manipulated by polarization optics and need only very few interferences; as opposed to the standard linear-optics cluster schemes, where complicated interferometry is always sensitive to losses and reduces the stability of the implementation.

Experimentally, we have verified that the cluster state setup suggested in scheme 1 can actually be implemented. The experimental realization is depicted in Fig. 3. A shot-noise limited ORIGAMI laser (Onefive GmbH) emitting 220 fs pulses

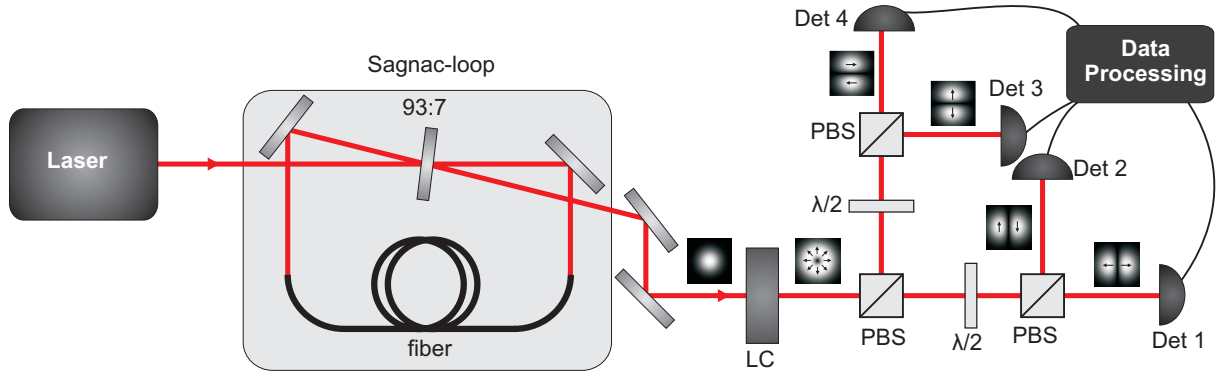


FIG. 3. The experimental setup to generate the cluster state from scheme 1 and measure the amplitude quantum correlations between the different modes. This scheme shows the case where a quadrature squeezed radially polarized beam enters the cluster-state generation circuit. By simply modifying the liquid crystal [LC], also an azimuthally polarized beam can be generated, while the passive circuit remains the same. [polarizing beam splitter (PBS), half-wave plate ($\lambda/2$)]

centered at 1560 nm acts as the light source. The light is injected into an asymmetric Sagnac interferometer [25] and generates an amplitude squeezed linearly polarized Gaussian mode. The key components of the Sagnac loop are a 93:7 beam splitter and a $6.45 \text{ m} \pm 0.02 \text{ m}$ long polarization maintaining single-mode fiber (3M FS-PM-7811) which acts as the nonlinear medium. The Gaussian output mode displays an amplitude squeezing of $-3.3 \text{ dB} \pm 0.1 \text{ dB}$ at a sideband frequency of 10.2 MHz. To realize scheme 1, one needs either a quadrature squeezed azimuthally or radially polarized mode. The radially polarized mode is obtained by mode transforming the Gaussian mode with the help of a liquid-crystal polarization converter (ARCOptix) and wave plates [24]. The losses at the device are $17\% \pm 0.5\%$ and we have measured $-1.9 \text{ dB} \pm 0.1 \text{ dB}$ squeezing in both the radially and azimuthally polarized mode. In the next step, the cylindrically polarized mode goes through a cascade of PBSs and half-wave plates, as indicated in Fig. 1a. The four outputs of the circuit are detected by single detectors with sub-shot noise resolution at a sideband frequency of 10.2 MHz.

The experimental scheme allows one to observe the amplitude quantum correlations present between the different modes. Table I lists all the different correlations and anti-correlations between the different output modes and their expected theoretical values. The excellent agreement between the theory and the experimental results shows that our passive circuit works near-perfectly and that it is capable of generating cluster states. It should be noted that in order to fully characterize the system and directly verify the entanglement contained in the cluster, more elaborate measurements are necessary. These will be part of further investigations.

In conclusion, we have demonstrated that quadrature squeezed cylindrically polarized modes are ideal tools to generate CV cluster states in a compact fashion. The intrinsic entanglement contained within these modes allows for a straightforward and easy generation of cluster states, therefore greatly reducing the complexity of the generation of

Correlations	Radially [dB]	Azimuthally [dB]
H01+H10	-0.8 (-0.8)	-0.9 (-0.8)
H01+V10	-0.8 (-0.8)	-0.9 (-0.8)
V01+H10	-0.8 (-0.8)	-0.8 (-0.8)
V01+V10	-0.7 (-0.8)	-0.8 (-0.8)
H01+V01	-0.8 (-0.8)	-0.9 (-0.8)
V10+H10	-0.7 (-0.8)	-0.8 (-0.8)
H01-H10	0.0 (0.0)	0.0 (0.0)
H01-V10	0.0 (0.0)	0.0 (0.0)
V01-H10	0.1 (0.0)	0.0 (0.0)
V01-V10	0.1 (0.0)	0.0 (0.0)
H01-V01	0.1 (0.0)	0.0 (0.0)
V10-H10	0.0 (0.0)	0.0 (0.0)

TABLE I. The amplitude correlation measurements between the different modes of the generated cluster states for either the radially or the azimuthally polarized mode as the input mode. The expected theory value is displayed in brackets. The experimental error is always $\pm 0.1 \text{ dB}$.

such states. As each node of the cluster state is a unique mode, these can be easily addressed individually, as needed for measurement-based quantum computations. We have also shown that our approach is versatile and can be exploited to obtain qualitatively different kinds of cluster states, including a fully connected, fully symmetric graph of four optical modes. The protocols proposed here clearly demonstrate that a combination of different polarization states and higher-order spatial modes, realizing a kind of hybrid entanglement of different degrees of freedom, leads to very compact and well addressable cluster states. These are crucial features for a realistic implementation of quantum computing with cluster states, and indeed, our system is easily scalable by utilizing higher-order TEM_{nm} modes. With regards to a complete scalability to large CV cluster states and computations, besides achieving compactness and addressability of the opti-

cal system, one issue remains, namely how to suppress finite-squeezing-induced errors.

We would like to acknowledge financial support from the European Union Integrating Project Q-ESSENCE. Peter van Loock wants to acknowledge funding by an Emmy Noether Grant of the DFG.

* These authors contributed equally to this work.

† Christoph.Marquardt@mpl.mpg.de

- [1] C. H. Bennett and D. P. DiVincenzo, *Nature* **404**, 247 (2000).
- [2] R. Raussendorf and H. J. Briegel, *Phys. Rev. Lett.* **86**, 5188 (2001).
- [3] R. Raussendorf, D. Browne, and H. J. Briegel, *Phys. Rev. A* **68**, 022312 (2003).
- [4] M. A. Nielsen, *Phys. Rev. Lett.* **93**, 040503 (2004).
- [5] P. Walther, K. J. Resch, T. Rudolph, E. Schenck, H. Weinfurter, V. Vedral, M. Aspelmeyer, and A. Zeilinger, *Nature* **434**, 169 (2005).
- [6] M. Van den Nest, A. Miyake, W. Dür, and H. J. Briegel, *Phys. Rev. Lett.* **97**, 150504 (2006).
- [7] N. C. Menicucci, P. van Loock, M. Gu, C. Weedbrook, T. C. Ralph, and M. Nielsen, *Phys. Rev. Lett.* **97**, 110501 (2006).
- [8] J. Zhang and S. L. Braunstein, *Phys. Rev. A* **73**, 032318 (2006).
- [9] X. Su, A. Tan, X. Jia, J. Zhang, C. Xie, and K. Peng, *Phys. Rev. Lett.* **98**, 070502 (2007).
- [10] N. C. Menicucci, S. T. Flammia, H. Zaidi, and O. Pfister, *Phys. Rev. A* **76**, 010302(R) (2007).
- [11] N. C. Menicucci, S. Flammia, and O. Pfister, *Phys. Rev. Lett.* **101**, 130501 (2008).
- [12] M. Pysher, Y. Miwa, R. Shahrokhshahi, R. Bloomer, and O. Pfister, *Phys. Rev. Lett.* **107**, 030505 (2011).
- [13] P. van Loock, C. Weedbrook, and M. Gu, *Phys. Rev. A* **76**, 032321 (2007).
- [14] O. Pinel, P. Jian, R. M. de Araújo, J. Feng, B. Chalopin, C. Fabre, and N. Treps, *Phys. Rev. Lett.* **108**, 083601 (2012).
- [15] M. Yukawa, R. Ukai, P. van Loock, and A. Furusawa, *Phys. Rev. A* **78**, 012301 (2008).
- [16] N. C. Menicucci, X. Ma, and T. Ralph, *Phys. Rev. Lett.* **104**, 250503 (2010).
- [17] N. C. Menicucci, *Phys. Rev. A* **83**, 062314 (2011).
- [18] T. G. Euser, M. A. Schmidt, N. Y. Joly, C. Gabriel, C. Marquardt, L. Y. Zang, M. Förtsch, P. Banzer, A. Brenn, D. Elser, M. Scharrer, G. Leuchs, and P. St.J. Russell, *J. Opt. Soc. Am. B* **28**, 193 (2010).
- [19] C. Gabriel, A. Aiello, W. Zhong, T. G. Euser, N. Y. Joly, P. Banzer, M. Förtsch, D. Elser, U. L. Andersen, C. Marquardt, P. St.J. Russell, and G. Leuchs, *Phys. Rev. Lett.* **106**, 060502 (2011).
- [20] B. dos Santos, K. Dechoum, and A. Khoury, *Phys. Rev. Lett.* **103**, 230503 (2009).
- [21] M. Lassen, G. Leuchs, and U. L. Andersen, *Phys. Rev. Lett.* **102**, 163602 (2009).
- [22] H. J. Briegel and R. Raussendorf, *Phys. Rev. Lett.* **86**, 910 (2001).
- [23] N. C. Menicucci, S. Flammia, and P. van Loock, *Phys. Rev. A* **83**, 042335 (2011).
- [24] A. Holleczek, A. Aiello, C. Gabriel, C. Marquardt, and G. Leuchs, *Opt. Express* **19**, 9714 (2011).
- [25] S. Schmitt, J. Ficker, M. Wolff, F. König, A. Sizmann, and G. Leuchs, *Phys. Rev. Lett.* **81**, 2446 (1998).